

Two-phase flow patterns in adiabatic refrigerant flow through capillary tubes

Luka Lorbek*, Anja Kuhelj, Matevž Dular, Andrej Kitanovski

*Laboratory for Refrigeration and District Energy, University of Ljubljana, Faculty of Mechanical Engineering, Ljubljana, Slovenia. luka.lorbek@fs.uni-lj.si (+38614771218)

Abstract:

This paper presents the results of an experimental study of the flow visualization of the refrigerant R600a through a capillary tube with an internal diameter of 0.8 mm made from an FEP (fluorinated ethylene propylene) polymer that was installed in a small-scale vapor-compression refrigeration system. The main purpose of the study was to determine the flow patterns of the refrigerant flow in capillary tubes under different operating conditions and to verify whether the results obtained using an FEP tube are representative for the flow of a refrigerant in copper capillary tubes. The results of the study revealed that the two-phase refrigerant flow in the FEP capillary tubes consists predominantly of a heterogenous flow composed of slugs, which continuously expand downstream. It was also found that at higher inlet pressures the frequency at which the vapor inception occurs is higher than at lower pressures. In addition, an experimental study of the effect of local or global imperfections on the inner surface of the FEP tube was performed. In some cases, the imperfections increased the number of vapor bubble inception points, which caused a homogenization of the two-phase flow.

Keywords:

Vapor-compression system, refrigerant flow, capillary tube, flash evaporation, flow visualization

Nomenclature:

Symbols:

G	mass flow rate [kg s ⁻¹]
p	pressure [Pa]
x	coordinate axis [m]
t	time [s]

Abbreviations:

EEV	electronic expansion valve
FEP	fluorinated ethylene propylene
FPS	frames per second
ID	internal diameter
PID	proportional integral derivative
RPM	revolutions per minute
RTD	resistance temperature detector

1. Introduction

Refrigerant flow in capillary tubes has attracted the interest of many researchers due to its complexity and its effect on the overall performance of vapor-compression refrigeration systems. Many of their works can be found in literature reviews such as Schulz (1985), Khan et.al. (2009) and Dubba et.al. (2017). Unlike electronic expansion valves (EEVs) capillary tubes have no moving parts and are very simple in terms of design. This makes them inexpensive compared to EEVs (Arora, 2009). The downside is that they are not able to actively regulate the flow of the refrigerant to the evaporator and therefore cannot adjust to varying load conditions (Melo et.al., 1999). They are commonly used in smaller vapor-compression systems such as household refrigerators, where the operating conditions do not change significantly. In such cases the capillary tubes can perform as well as EEVs (Marcinichen and Melo, 2006). In a refrigeration system their purpose is to decrease the pressure of the condensed refrigerant below the saturation pressure. At this point the refrigerant will start to evaporate and expand. Consequently, its temperature will decrease. This low-temperature refrigerant, whose mass flow rate is controlled by the capillary tube, will then flow to the evaporator where it can absorb the heat from the thermal source. The pressure drop in a capillary tube is the result of the large friction forces acting on the fluid due to the small diameter and thus a higher relative roughness. It is also caused by the continuous acceleration of the fluid due to a decreasing density caused by the gradual increase of the vapor fraction. This process of adiabatic evaporation is a very complex phenomenon. It involves turbulent, two-phase, phase-changing, compressible flow. A delay in vaporization, called the metastable flow, can also occur (Pascua, 1953, Cooper et.al., 1957, Li et.al., 1990). To better understand the two-phase flow in capillary tubes several researchers have performed different refrigerant-flow visualization studies. Cooper et.al. (1957) were among the first to describe the two-phase refrigerant flow as a “fog flow” while studying the delay of vaporization in glass capillary tubes. In their study Mikol and Dudley (1964) used a stroboscope in order to visualize the flow of R12 in a glass capillary tube. Their results showed an intense bubbly flow and sometimes an annular flow that formed a vapor core surrounded by liquid. Near the outlet of the capillary tube the flow was described as a “uniform spray of liquid droplets borne by vapor”. Koizumi and Yokoyama (1980) performed an investigation of the flow of the R22 refrigerant through a capillary tube made of Pyrex glass with an inner diameter of 1.0 mm. At the point of inception, the bubbles were seen to grow and combine, whereas at the outlet of the capillary tube the flow was described as a “homogeneous” bubbly flow. By visualizing the refrigerant flow of R404A Motta et al. (2002) studied whether the concentration of the compressor oil has an effect on the delay of vaporization in a capillary tube. By changing the oil concentration, they managed to influence the vaporization point. They described the flow as a fog-like flow. Martinez-Ballester et al. (2017) performed a visualization of the flow of R600a at the inlet of the capillary tube in a household refrigerator. They showed that despite the refrigerant being in a subcooled state vapor was still present and was being continuously drawn into the capillary tube along with the liquid. After the initial studies in the 1950s and 60s, little attention has been given to the visualization of refrigerant flow in capillary tubes. As such the flow of refrigerant through capillary tubes has been commonly viewed as a homogenous bubbly/misty flow, especially in studies related to the mathematical modeling of the refrigerant flow (Sami and Maltais, 2000, Xu and Bansal, 2002, Bansal and Rupasinghe, 1998, Bullard and Jain, 2004, Heimel et.al., 2012, Wongwises and Pirompak, 2001, Agrawal and Bhattacharyya, 2007). Due to advances in photographic and lighting technologies Tannert and Hesse (2016) noticed different flow patterns, such as plug flow at the capillary tube’s outlet, while examining the noise effects caused by refrigerant flow in the capillary tube of a household refrigerator. Such a flow pattern indicates the presence of a heterogeneous flow. A number of mathematical models of capillary tubes (Garcia-Valladares, 2007, Wang et.al, 2012, Seixlack and Barbazelli, 2009, Seixlack, 1996) that are based on the separated two-phase flow model where the flow is assumed to be heterogeneous can be found in the literature. The results reported in these studies agree slightly better with the experimental results compared to homogeneous models, but several studies (Furlong and Schmidt, 2012, Wong and Ooi,

1996) point out that both two-phase models can be used to describe the flow of refrigerants in capillary tubes. Although homogeneous and separated flow models have been compared extensively with each other and against experimental data, no investigation, at least to the best of the authors' knowledge, has been made to experimentally determine the velocity ratio of the vapor and liquid phases, which is one of the key parameters that indicate the homogeneity of the flow. Therefore, we decided to investigate the flow of R600a through a capillary tube installed in a small-scale vapor-compression refrigeration system. The primary goal was to observe the flow patterns in the two-phase region of the capillary tube flow from which an attempt would be made to determine the velocity ratio. Because the capillary tube that was used to enable the visualization of the flow was made from an FEP polymer the second part of the study focused on the effects of two different surface-texture properties. The goal was to try and determine whether, or to what extent, the flow patterns in an FEP capillary tube are representative of the flow in a copper capillary tube that is actually used in vapor-compression systems.

2. Experimental set-up

To ensure similar flow conditions to those in real applications and to be able to control and regulate them, an experimental vapor-compression refrigeration system was set up. The system was designed to mimic the operation of a real household refrigerator, charged with the refrigerant R600a. A scheme of the set-up is shown in Fig. 1.

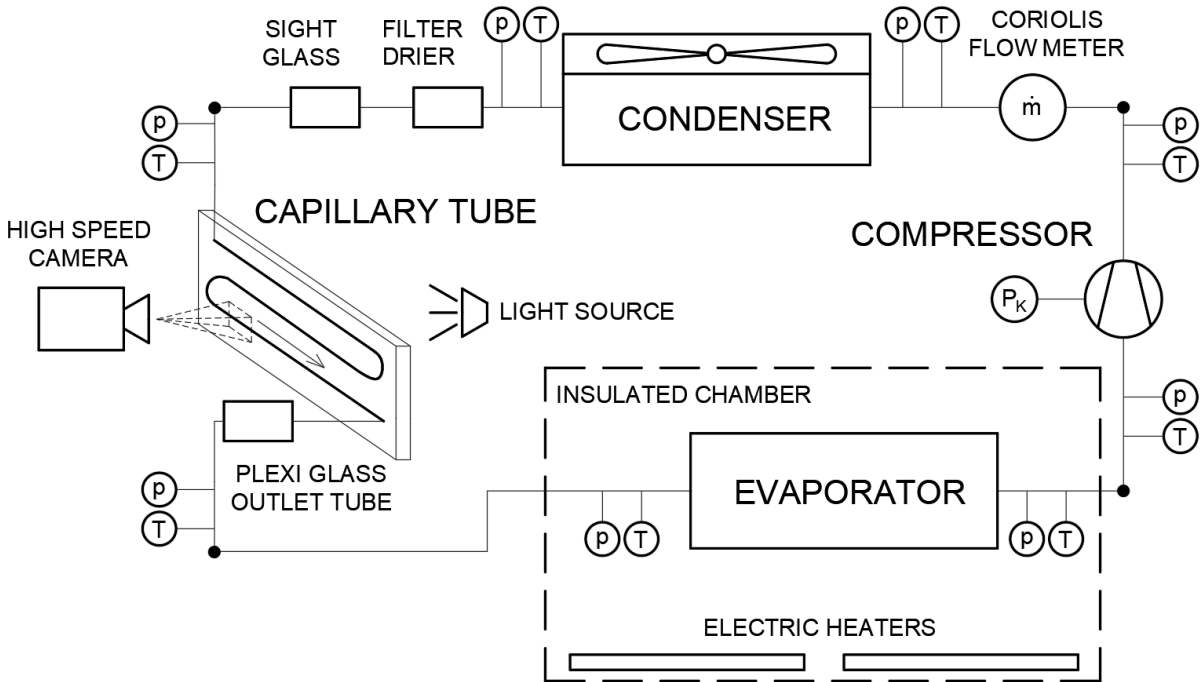


Fig 1: Schematic of the experimental set-up.

The refrigeration system comprises a variable-speed piston compressor connected to a Coriolis mass-flow meter and a dynamic condenser. A sight glass and a filter drier are positioned after the condenser. Connected to these is the test section for capillary tubes that enables the simultaneous installation of up to two capillary tubes. The capillary tube is inserted into a plexi-glass tube which enables the visualization of the flow at the outlet. A static evaporator is located inside an insulated cabinet. Pressure and temperature measurements are taken at the inlet and outlet of each main component. Two electric heaters control the air temperature in the cabinet via a PID (proportional-integral-derivative) controller connected with an RTD (resistance temperature detector). The PID controller is also connected with one

pressure sensor on the condensing side and one on the evaporating side. The pressure at the inlet of the capillary tube can be regulated by varying the condenser fan's RPMs. By increasing the rotational speed of the fan heat transfer to the surroundings will increase. Consequently, the condensing pressure and the pressure at the capillary tube inlet will decrease. In most cases the pressure at the outlet of the capillary tube is independent of the downstream conditions because the flow at the outlet is choked. If the flow is not choked, the pressure at the outlet of the capillary tube or rather the evaporating pressure can be regulated by increasing or decreasing the RPMs of the compressor. Higher RPMs will result in a higher mass flow rate which will cause the pressure in the evaporator to decrease and vice versa. This however would cause the mass flow rate through the capillary tube to slightly fluctuate. This was deemed inappropriate for this study as we needed to achieve stable evaporating conditions in the capillary tube. Therefore, the mass flow rate or rather the compressor RPMs were kept constant during a specific measurement.

The system can also operate at constant compressor and fan RPMs to ensure a steady mass flow rate of refrigerant and air, respectively.

The refrigerant flow in the capillary tube was observed with a high-speed camera. The camera was positioned parallel to the capillary tube, which was attached to a Plexiglass plate. An LED was placed behind the glass plate to illuminate the flow. Because we wanted to observe the refrigerant flow along the entire length of the capillary tube, which can be up to a few meters, it was unpractical to make the capillary tube from glass. Therefore, a transparent FEP polymer tube with an internal diameter of 0.8 mm, an external diameter of 1.6 mm and a length of 3.1 m was selected as our capillary tube. FEP is a polymer commonly used in capillary electrophoresis and has a high chemical inertness towards most chemicals (Sahlin, 2002). This property is important because the refrigerant must not dissolve the polymer. Otherwise the refrigerant could become contaminated or could eventually damage the wall of the capillary tube. For this reason, preliminary tests were carried out on the effect of the exposure of the polymer to the refrigerant. The refrigerant was in contact with the polymer for three weeks and the tube did not show any noticeable signs of reaction or change. As the mass flow rate was measured after the compressor all the measurements were performed after the system reached a steady state, when the mass flow rates through the capillary tube and the compressor were equalized. Table 1 contains the information about the measuring equipment that was used in the experiment.

Table 1: Measuring equipment and features.

	Type/Range	Accuracy
Pressure transmitters	Pressure transmitter 0...25 bar (absolute)	$\pm 0.3\%$ of measurement range (± 0.08 bar)
	Pressure transmitter -1...12 bar (relative)	$\pm 0.3\%$ of measurement range (± 0.04 bar)
Thermocouples	K-type	± 0.2 K (calibrated)
Coriolis mass flow meter	0...90 kg h ⁻¹	> 4 kg h ⁻¹ ... < 0.5% of measured value < 4 kg h ⁻¹ ... < 1.5% of measured value
	Properties	
High-speed camera	1.3 Megapixels 1280 × 1024 resolution at 2000 FPS Flow observed at 20000 and 32000 FPS (1280 × 152)	

3. Results and discussion

3.1. Performance comparison of the FEP and the copper capillary tube

Whereas most researchers who performed visual studies utilized glass capillary tubes, in our study the capillary tube was made of fluorinated ethylene propylene (FEP). Since the flow behavior with respect to the transparent FEP and copper tubes could differ, the first step in the experimental analysis was to evaluate the operating conditions for the same geometry of both capillary tubes in a vapor-compression system. For the purpose of the study, an FEP and a copper capillary tube with an internal diameter of 0.8 mm and a length of 2 m were installed in the experimental set-up. The mass flow rate and pressure drop were measured for different compressor RPM ranging from 30% to 100% of the nominal value. The mass flow rate at which the system reaches steady-state conditions does not differ between the FEP and copper capillary tubes when increasing the compressor RPMs. A difference of around 5% can be noticed only when the flow approaches choked conditions. In this case for the same inlet conditions the FEP capillary tube can provide a slightly larger mass flow rate than the copper tube. Likewise, the pressure drop did not vary by more than $\pm 2\%$ at different mass flow rates. The refrigerant charge and the inlet pressure were kept equal in both test cases. At low compressor RPMs the subcooling degree varied by a maximum of 0.7 K or around 18% of the absolute subcooling degree. This was due to the lack of a mechanism that could regulate a constant subcooling. Nonetheless, the result shows that in terms of pressure drop, which is an indicator of the surface roughness, the FEP capillary tube has similar properties to a copper capillary tube.

3.2. Inception of vaporization

In their research on glass capillary tubes Mikol and Dudley (1964) reported that the inception of vaporization always occurred at one point on the tube wall, never around the entire circumference and never in the entire cross-section of the flow. This agrees with our observations. The vaporization always occurred at a single point on the lower part of the tube wall. We emphasize that even though the vaporization point did not change the absolute values on the gridlines of different figures can be different as the camera was moved around during different shots. Fig. 2 shows an example of the bubble formation at the inception point. The scale on the figure marks the outer diameter and the dotted lines indicate the tube interior. The white circle indicates the inception point. Small bubbles rise from the surface of the tube in groups of 1 to 4 bubbles, depending on the operating conditions. They then quickly merge into larger bubbles that are carried downstream by the liquid refrigerant. The bubbles begin to expand in the direction of the flow. Probably because the pressure downstream is lower than the pressure upstream. Therefore, its growth is less restricted in the direction of the flow. The bubbles also begin to accelerate and transform into slugs.

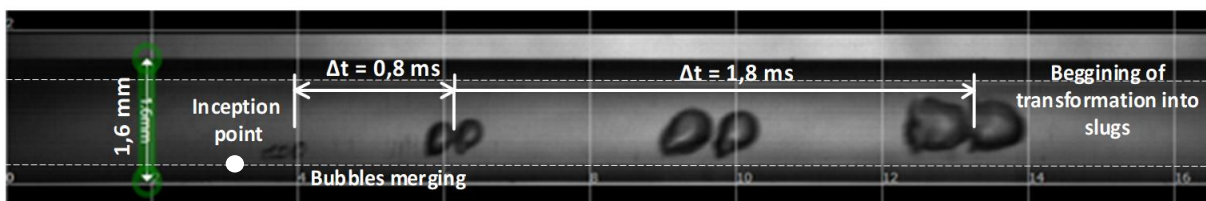


Fig 2: Vapor slug formation at inlet pressure of 6.1 bar and mass flow rate of 2.5 kg h⁻¹.

The frequency at which these bubble bursts appear increases with increasing inlet pressure and remains more or less constant along the capillary tube's length. Downstream of the point of inception, as shown later in Fig. 7, the small bubbles no longer exist but merge into a single slug. It is possible to assume that a constant frequency along the length of the capillary tube means that although the smaller bubbles from one group burst merge into a slug, the slugs themselves do not merge with each other. No explanation was found as to why the frequency increases with a larger inlet pressure. Figs. 3-4 depict

the inception of vapor bubbles and their transformation into slugs for two more operating conditions where the mass flow rate was varied from 2.2 kg h⁻¹ to 2.4 kg h⁻¹. The inlet pressure was varied from 4.7 bar to 5.3 bar.

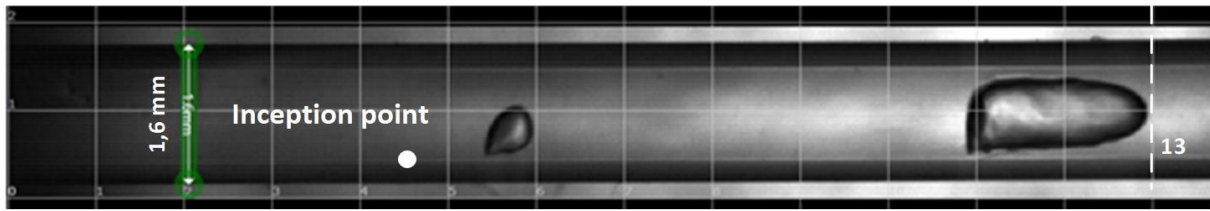


Fig 3: Vapor slug formation at inlet pressure of 4.7 bar and mass flow rate of 2.2 kg h⁻¹.

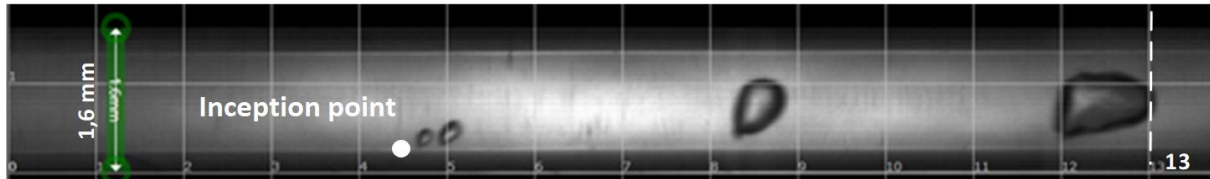


Fig 4: Vapor slug formation at inlet pressure of 5.3 bar and mass flow rate of 2.4 kg h⁻¹.

From Figs. 2-4 we can see that different operating conditions can affect the shape of the formed slugs, the frequency at which they appear, and their velocity. In Fig. 3 the single vapor bubble is already transformed into a slug at the 13-mm grid mark, having expanded downstream as its rear was pushed on by the liquid. At this point, the shape of the slug resembles a so-called Taylor bubble (Taylor, 1960). In Fig. 2 bursts of smaller bubbles are still joining together into larger bubbles. This can perhaps be attributed to the pressure of the liquid phase surrounding the bubble, which restricts its expansion. In Fig. 2 the liquid enters the capillary tube at a higher pressure than in the case shown in Fig. 3, which means that at the point of inception the pressure acting on the bubble in Fig. 2 is larger than in Fig. 3. This higher pressure could dampen the bubble's expansion. The average velocity of the vapor phase increases from 3.1 m s⁻¹ in Fig. 3 to 3.3 m s⁻¹ in Fig. 4 and to 3.7 m s⁻¹ in Fig. 2 due to the increase of the mass flow rate. The vapor slugs have a shape that resembles the pattern of vertical slug flow in a tube (Weisman, 1983) even though the tube was faced horizontally. We believe that this is due to the high velocity of the flow and the small diameter of the tube.

3.3. Flow patterns along the distance of the capillary tube

The following figures depict an example of the two-phase flow patterns observed at discrete points along the capillary tube. A coordinate axis x with a positive direction towards the capillary tube outlet was used to mark the different locations where the flow was observed. The outlet of the capillary tube is located at $x = 50$ cm and $x = 0$ is a point 50 cm upstream from the outlet. The inlet pressure was set to 4.7 bar and the mass flow rate through the capillary tube was 2.2 kg h⁻¹. Fig. 5 depicts the starting point of the vaporization. The bubbles form on the lower wall and begin expanding into a slug (see also Fig 3).

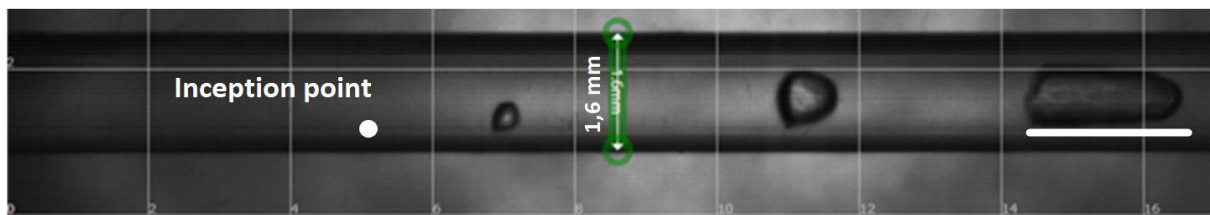


Fig 5: Point of vapor inception. Bubbles begin forming into slugs ($x = 25.5$ cm).

The slug (underlined with a white line in Figs. 5 and 6) expands very quickly, increasing in size from $L = 2\text{ mm}$ in Fig. 5 ($x = 25.5\text{ cm}$), to $L = 14\text{ mm}$ ($x = 28\text{ cm}$), as shown in Fig. 6.

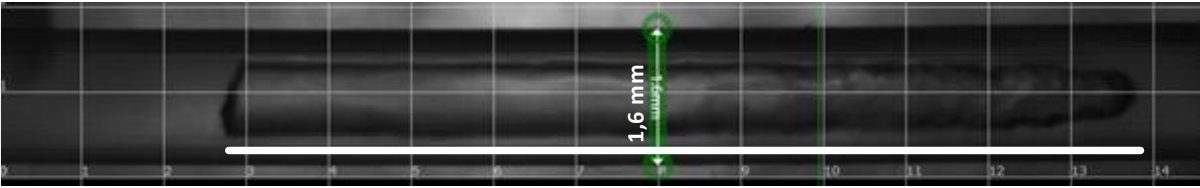


Fig 6: Slugs expanding downstream ($x = 28\text{ cm}$).

By $x = 32\text{ cm}$ in Fig. 7 the slugs that formed from bubbles from the same bubble burst begin to merge with each other because their front-end velocities are much higher than their rear-end velocities. The difference in the velocity is shown later in Fig. 10.

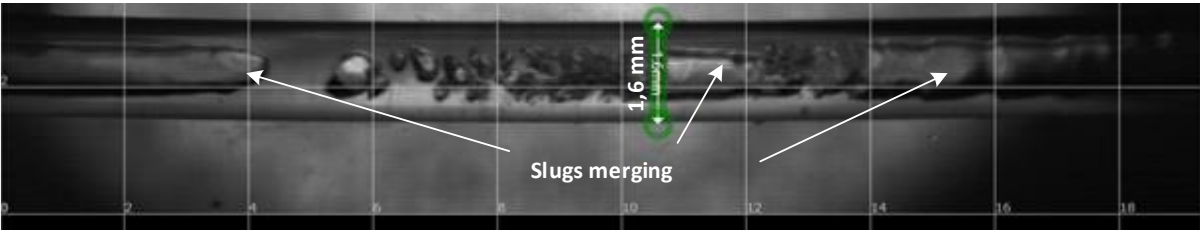


Fig 7: Slugs from the same bubble burst begin to merge ($x = 32\text{ cm}$).

After merging in Fig. 7 the slug shown in Fig. 8 (at $x = 42\text{ cm}$) continues to expand and accelerate. However, it is now followed by a patch of mist. This misty patch is attached to the slug and seems to be formed of small vapor bubbles. The refrigerant vapor flows as this continuous slug until the outlet of the capillary tube. The slug on Fig. 8 is split into two parts because we were unable to fit the entire slug into one frame.

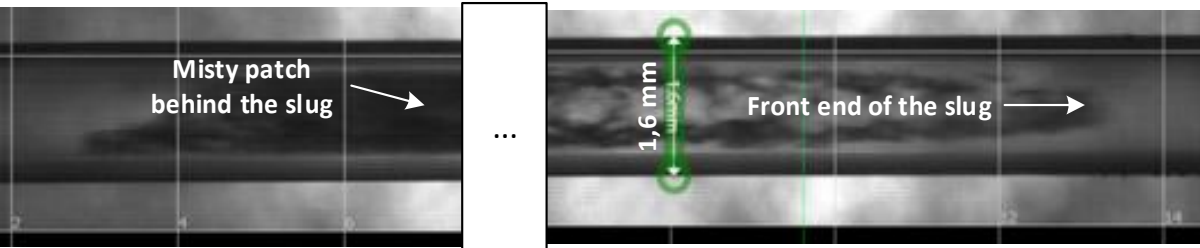


Fig 8: Misty patches follow the slug ($x = 42\text{ cm}$).

Most vapor-compression systems have their capillary tube inserted and soldered straight into the evaporator tube. We tried to recreate this geometry by inserting the capillary into a $15 \times 15\text{ mm}$ plexi-glass block with an internal tube of 5 mm , as shown in Fig. 9. The contact between the tube and plexi-glass was minimized as much as possible to prevent heat transfer having a significant effect on the refrigerant flow. The flow at this location was hard to visualize, but from our observations we conclude that after the refrigerant flows out of the capillary tube the liquid phase is forced against the tube wall as the vapor core expands into the tube. When the misty rear end of the slug that is shown in Fig. 8 (bottom) exits the capillary it fills the tube with tiny bubbles for a brief moment before the vapor core again starts pressing the liquid against the tube wall.

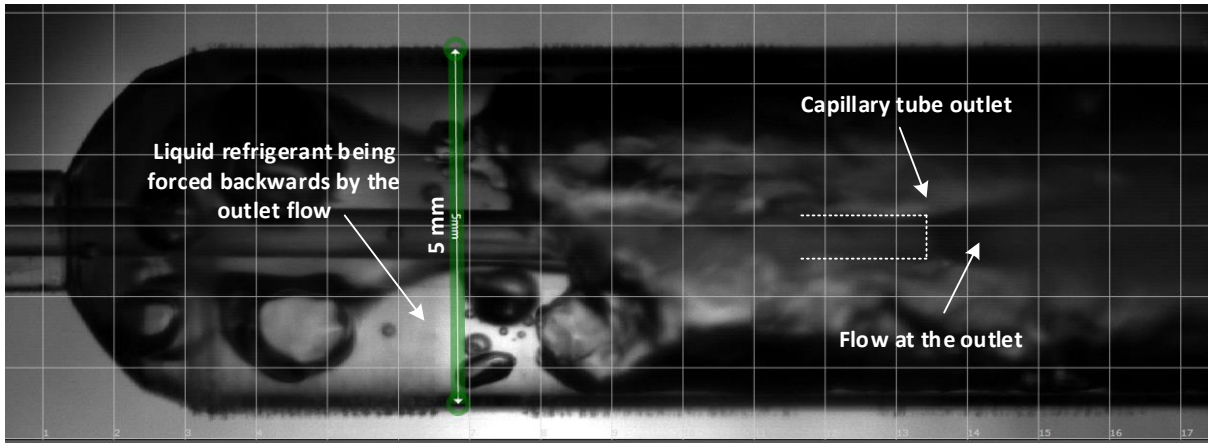


Fig 9: Refrigerant flow at the capillary tube's outlet.

3.4. Velocity of the vapor phase

Fig. 10 shows the velocities of the front and rear ends of the vapor phase along the capillary tube's length for the conditions described in the previous section. The x-axis locations were translated into the real positions with respect to the entire length of the capillary tube. The velocity was measured and averaged for three different bubbles/slugs. The vapor phase accelerates downstream from around 3 m s^{-1} at the point of inception up to around 20 m s^{-1} towards the outlet. The velocity is slightly higher for greater inlet pressures. It is also apparent that the front end of the vapor formation is faster than its rear end. This confirms our observation that the slugs expand downstream and continue to do so until the outlet.

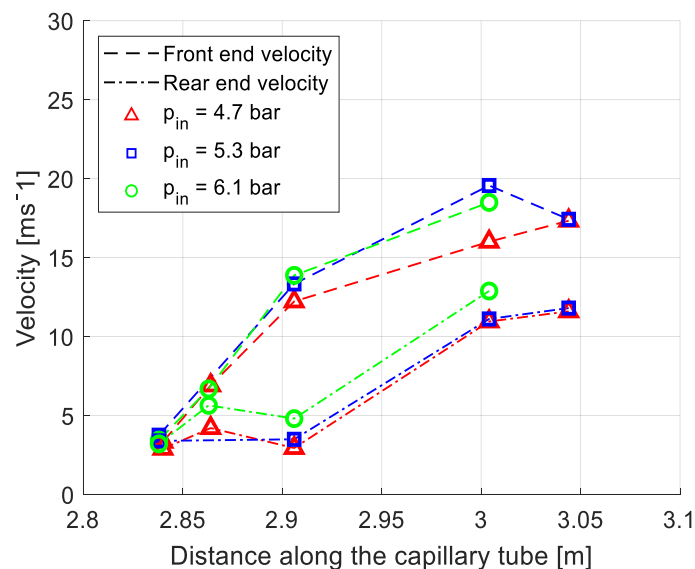


Fig 10: Velocities of the front and rear ends of the vapor phase along the capillary tube's length.

The velocity of the vapor phase is relatively simple to determine because the vapor patterns can be clearly seen and the distances that they travel in a certain period of time are clear. However, the liquid velocity cannot be determined visually because no visible patterns can occur. Methods such as particle image velocimetry (PIV) would be needed to determine the velocity of the liquid phase. This would require adding solid particles to the flow without allowing them to clog up the capillary tube and preventing air from breaching the system while adding them. This is without a doubt a challenge in itself

and is beyond the scope of this work. However, the velocity of the liquid phase can still be estimated to some degree. For example, at the rear end of a bubble or slug. There the liquid and vapor velocities are probably similar as the overall vapor fraction in a capillary tube is low and it is the liquid that is carrying the bubble or pushing the vapor slug downstream. Although not a perfectly representative value of the liquid velocity, the rear-end velocity of the vapor phase can be clearly determined and no intrusive method is needed. From the results shown in Fig. 10 it is then possible to obtain the ratio between the front- and rear-end vapor velocities. Again, while that is not an absolutely correct value it is nevertheless an indicator of the velocity slip between the liquid and vapor phases. The front/rear velocity ratio is close to unity only at the point of inception. There the small bubbles are carried by the liquid and the velocities of the two phases are very similar. As the vapor phase expands its velocity begins to exceed the liquid velocity and the ratio increases. Towards the outlet of the capillary tube the vapor phase expands at a slower rate than after the inception and the front/rear velocity ratio decreases. The main conclusion is that the velocity of the vapor phase is not uniform. If the liquid velocity is uniform ahead of and behind a vapor slug, and is more similar to the velocity of the rear end of the slug, then the velocities of the vapor and liquid phases are quite different for most of the two-phase region. In that case, the two-phase flow of a refrigerant in an FEP capillary tube cannot be considered as homogeneous.

4. Effect of surface imperfections on two-phase refrigerant flow

The question now arises as to whether the flow patterns described in the previous sections are representative of what happens in copper capillary tubes that are actually used in vapor-compression refrigeration systems. We described the similarity between the FEP and the copper capillary tube based on a comparison of the inlet and outlet conditions. As the internal diameter and length were equal a similar pressure drop at the same compressor RPMs shows that the surface effects of both tubes have a similar overall influence on the refrigerant flow. However, this does not prove that the two-phase flow patterns remain the same as a similar pressure drop could coincidentally be caused by a different type of flow. Consequently, our observation that the flow is not homogeneous might not be true for copper capillary tubes. The surface roughness of copper capillary tubes depends on the production process and different researchers have reported surface roughness values from $0.05\ \mu\text{m}$ up to $11\ \mu\text{m}$ (Meyer and Dunn, 1996). However, a copper capillary tube is considered to have more imperfections than a glass capillary tube (Mikol and Dudley, 1964). By this logic a copper surface is likely to produce more inception points for vapor bubbles. Mikol and Dudley (1964) reported that the inception of vaporization happened at a single point, which is equivalent to what happens in an FEP tube. We therefore assume that the FEP tube has a surface texture and properties that cause a similar effect to a glass capillary tube. Further investigations were performed to verify whether a surface texture with more imperfections (as is expected in a copper capillary tube) could influence the two-phase flow. Two different cases were considered. In the first case several local imperfections were created. In the second case the entire inner surface of the tube was grooved with a sharp spring steel wire. A macroscopic spiral groove was created and the sharp steel tip of the wire created microscopic abrasions on the surface. This enabled us to simultaneously observe both the macroscopic and microscopic influences on two-phase flow.

4.1. Effect of local imperfections

In all the experiments, when stable evaporating conditions were achieved, i.e., the capillary tube did not draw in vapor at the inlet, the inception of vaporization occurred at the same location, regardless of the inlet pressure or mass flow rate. The vapor bubbles originated from the lower tube wall, around 27 cm from the capillary tube's outlet. We introduced imperfections in the capillary tube by twisting it and slightly damaging its inner surface every 4 cm upstream and downstream of the current vaporization point for 8 cm in each direction (two points in each direction). Our intention was to disturb the metastable flow and force the onset of vaporization. The vaporization point jumped by 4 cm upstream of the current vaporization point and Fig. 11 shows how the vapor bubbles now form at this imperfection (see Figs. 2-5 for vaporization points in a tube without imperfections).

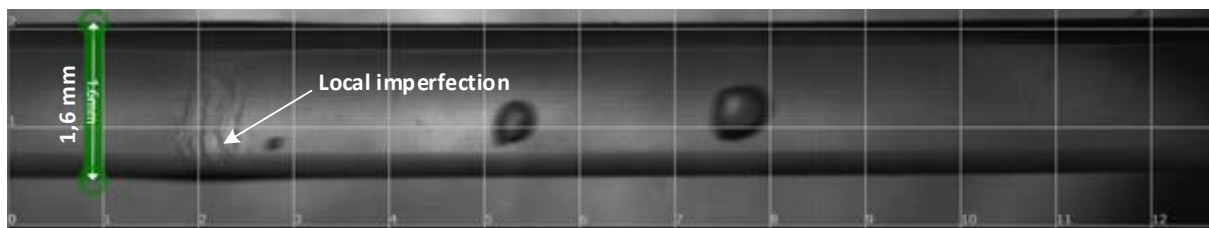


Fig 11: Inception of vaporization at a surface imperfection.

The earlier onset of vaporization did not have any significant effect on the overall operation of the system in terms of mass flow rate and pressure drop. After the introduction of these imperfections further changes to the inlet conditions did not move the starting point of the vaporization. The offset of the vaporization starting point did not affect the flow patterns that were presented in Figs. 5-9.

4.2. Effect of grooving and abrasions

In order to verify the effect of the surface texture on the flow patterns, spiral grooves and abrasions were created along the entire length (1.5 m) of the FEP tube. A non-contact optical profilometer was used to create a 3D profile of the surfaces from which a 2D profile (Fig. 12) could be determined for a representative section of the surface. The profile of the grooved tube in Fig. 12 has an amplitude of around 60 microns (the ID of the tube is 800 microns) at intervals of around 250 microns. The surface of the original tube has no macroscopic profile. The profilometer was unable to measure the profile below the micron level where microscopic abrasions might be visible.

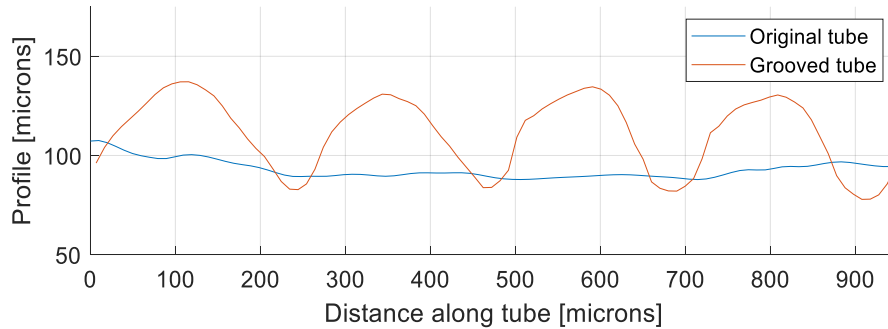


Fig 12: Surface profiles of samples taken from the original and grooved capillary tubes.

The grooving of the capillary tube resulted in several vaporization points (Fig. 13) scattered randomly around the circumference of the tube (compared to a single point in a smooth tube) when the compressor was operating at 100% of its nominal RPM. However, when the compressors' RPM were lowered to 60% of the nominal rate, the vaporization again occurred at only a single point like in Figs. 2-4. Because of the limited resolution of the high-speed camera we were not able to determine whether the increase in the number of vapor inception points is due to the microscopic abrasions, the macroscopic grooves, or both.

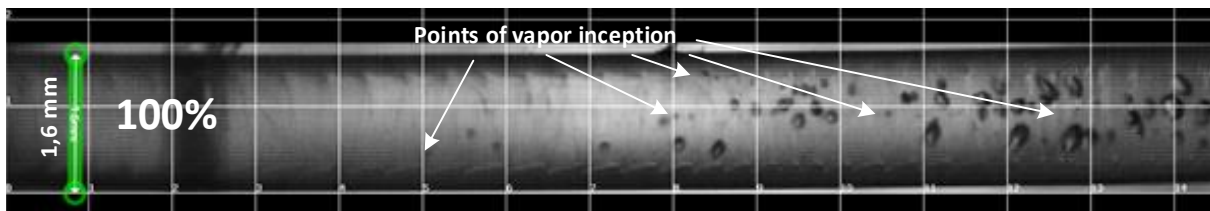


Fig 13: Inception at 100% of nominal compressor RPM.

The refrigerant flow was observed at discrete points along the capillary tube length, as in Figs. 5-9. The downstream evolution of the bubbles is depicted in Fig. 14, which shows different flow patterns established along the capillary tube. The compressors' RPM were set to 60% of the nominal rate in this case. At $x = 29$ cm (Fig. 14, top) we can see that the flow consists of slugs and smaller bubbles. It seems that either not every bubble can expand into a slug or that more bubbles form downstream from the first vapor-inception point. When the flow approaches the outlet, it becomes more homogenous and the vapor and liquid phases are no longer distinguishable from each other to the naked eye. This is shown in Fig. 14 (bottom).

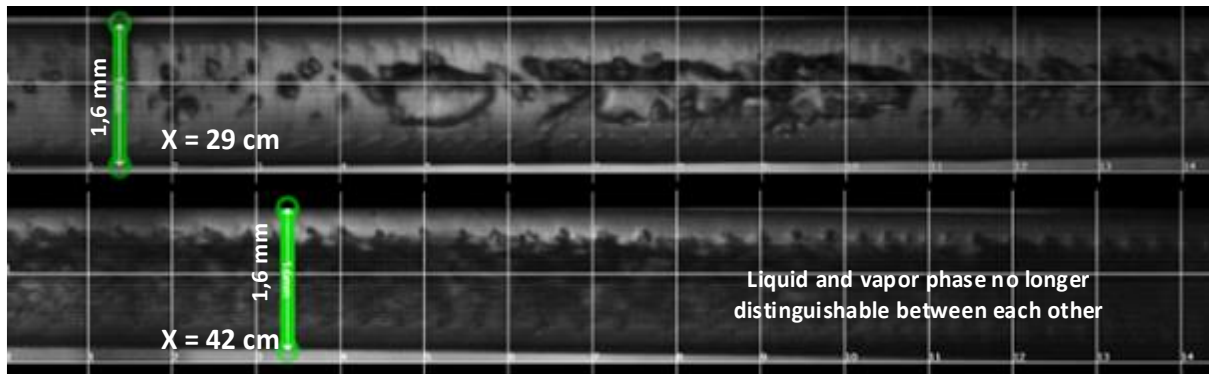


Fig 14: Top) vapor slugs and bubbles at $x = 29$ cm, bottom) homogeneous flow at $x = 42$ cm. The system was operating at 60% nominal compressor RPM.

From the results shown in this section we can conclude that a different surface texture has an effect on the homogeneity of the flow. Therefore, it is not clear whether the results obtained with a FEP capillary tube are representative for copper tubes as well. If the surface texture is smooth and similar to the surface of an FEP capillary tube, then the flow pattern will likely not be homogeneous as it will resemble the flow shown in Figs. 5-9. However, if the surface has many imperfections then it is possible that the flow in a copper capillary tube is more homogeneous due to the many bubbles forming on the entire circumference of the tube, as shown in Figs. 13 and 14.

5. Conclusions

In this article we reported on a visual study of the flow of the refrigerant R600a through a capillary tube made from an FEP polymer. The study showed that for a given geometry a higher inlet pressure led to a higher frequency of bubble formation and a smaller size of the bubbles. While traveling downstream, these bursts of bubbles then expanded into slugs and merged with each other into larger slugs, which continued to expand until the outlet of the capillary tube. The two-phase flow in the FEP capillary tube proved to be a predominantly slug flow followed by short misty patches of small bubbles towards the outlet of the tube. By visualizing the refrigerant flow along the entire length of the capillary tube it was possible to determine the velocity of the vapor phase as it continuously accelerated downstream. It was shown that the front end of the vapor phase has a higher velocity than the rear end. The ratio of the vapor phase front- and rear-end velocities exceeded 1.5 throughout most of the two-phase length in the capillary tube and even reached a value of 4 at certain locations. This indicates that the flow of the refrigerant is inhomogeneous. An investigation was made to determine whether the results of the study on an FEP capillary tube are representative of the flow in copper capillary tubes. Firstly, a comparison between the FEP capillary tube used in the study and a copper capillary tube was performed and the results showed a minimal difference in terms of the pressure drop ($\pm 2\%$) and the mass flow rate ($\pm 5\%$) through the tubes. Secondly, because a copper capillary tube is likely to have more imperfections than an FEP capillary tube we studied the effect of different imperfections on the two-phase flow patterns. Two cases were considered. In the first case we were able to discretely move the inception point of the vapor by 4 cm upstream of the existing point by creating a local imperfection. However, this did not affect the overall operation of the system and did not change the flow pattern. In the second case we created macroscopic grooves and microscopic abrasions on the entire inner surface of the tube. The results showed that the number of vapor-inception points increased and the flow downstream became more homogeneous. Because these surface imperfections have an effect on the inception of vapor bubbles and the homogeneity of the flow we cannot confirm whether the flow patterns found in an FEP capillary tube are representative of the flow in copper capillary tubes as well. Further studies will be necessary to determine whether the surfaces of the FEP and the copper capillary behave in a similar manner during flash evaporation.

6. References

- Agrawal, N., Bhattacharyya, S., 2007. Adiabatic capillary tube flow of carbon dioxide in a transcritical heat pump cycle. *Int. J. Energy Res.* <https://doi.org/10.1002/er.1294>
- Arora, C.P., 2009. Refrigeration and air conditioning, Third Edit. ed. Tata McGraw-Hill, New Delhi.
- Bansal, P.K., Rupasinghe, A.S., 1998. An homogeneous model for adiabatic capillary tubes. *Appl. Therm. Eng.* 18, 207–219.
- Bullard, C., Jain, G., 2004. Design and optimization of capillary tube- suction line heat exchangers, in: *International Refrigeration and Air Conditioning Conference*. Purdue, pp. 1–8.
- Cooper, L., Chu, C.K., Brisken, W.R., 1957. Simple selection method for capillaries derived from physical flow conditions. *Refrig. Eng.* 65, 37.
- Dubba, S.K., Kumar, R., 2017. Flow of refrigerants through capillary tubes: A state-of-the-art. *Exp. Therm. Fluid Sci.* 81, 370–381. <https://doi.org/10.1016/j.expthermflusci.2016.09.012>
- Furlong, T.W., Schmidt, D.P., 2012. A comparison of homogenous and separated flow assumptions for adiabatic capillary flow. *Appl. Therm. Eng.* 48, 186–193. <https://doi.org/10.1016/j.applthermaleng.2012.05.007>
- García-Valladares, O., 2007. Numerical simulation and experimental validation of coiled adiabatic capillary tubes. *Appl. Therm. Eng.* 27, 1062–1071. <https://doi.org/10.1016/j.applthermaleng.2006.07.034>
- Heimel, M., Lang, W., Berger, E., Almbauer, R., 2012. A homogenous capillary tube model - Comprehensive parameter studies using R600a, in: *International Refrigeration and Air Conditioning Conference*. Purdue.
- Khan, M.K., Kumar, R., Sahoo, P.K., 2009. Flow characteristics of refrigerants flowing through capillary tubes - A review. *Appl. Therm. Eng.* 29, 1426–1439. <https://doi.org/10.1016/j.applthermaleng.2008.08.020>
- Koizumi, H., Yokoyama, K., 1980. Characteristics of refrigerant flow in a capillary tube. *ASHRAE Trans.* 86, 19–27. [https://doi.org/10.1016/0029-5493\(93\)90092-N](https://doi.org/10.1016/0029-5493(93)90092-N)
- Li, R.-Y., Lin, S., Chen, Z.-Y., Chen, Z.-H., 1990. Metastable flow of R12 through capillary tubes. *Int. J. Refrig.* 13, 181–186. [https://doi.org/10.1016/0140-7007\(90\)90073-6](https://doi.org/10.1016/0140-7007(90)90073-6)
- Marcinichen, J.B., Melo, C., 2006. Comparative Analysis Between a Capillary Tube and an Electronic Expansion Valve in a Household Refrigerator, in: *Proceedings of the International Refrigeration and Air Conditioning Conference*. Purdue.
- Martínez-Ballester, S., Bardoulet, L., Pisano, A., Corberán, J.M., 2017. Visualization of refrigerant flow at the capillary tube inlet of a high-efficiency household refrigerator. *Int. J. Refrig.* <https://doi.org/10.1016/j.ijrefrig.2016.09.019>
- Melo, C., Ferreira, R.T.S., Boabaid Neto, C., Goncalves, J.M., Mezavila, M.M., 1999. An experimental analysis of adiabatic capillary tubes. *Appl. Therm. Eng.* 19, 669–684.
- Meyer, J.J., Dunn, W.E., 1996. Alternative Refrigerants in Adiabatic Capillary Tubes. Urbana. <https://doi.org/10.5935/0101-2800.20170053>
- Mikol, E.P., Dudley, J.C., 1964. A visual and photographic study of the inception of vaporization in adiabatic flow. *J. Fluids Eng. Trans. ASME* 86, 257–261. <https://doi.org/10.1115/1.3653052>
- Motta, S.F.Y., Parise, J.A.R., Braga, S.L., 2002. A visual study of R-404A/oil flow through adiabatic capillary tubes. *Int. J. Refrig.* 25, 586–596. [https://doi.org/10.1016/S0140-7007\(01\)00057-3](https://doi.org/10.1016/S0140-7007(01)00057-3)
- Pascua, P.F., 1953. Metastable flow of Freon-12. *Refrig. Eng.* 61, 1084–1088.
- Sahlin, E., 2002. Capillary zone electrophoresis in laboratory-made fluorinated ethylene propylene capillaries. *J. Chromatogr. A* 972, 283–287.
- Sami, S.M., Maltais, H., 2000. Numerical modeling of alternative refrigerants to HCFC-22 through capillary tubes. *Int. J. Energy Res.* 24, 1359–1371.
- Schulz, U.W., 1985. State of the art: The capillary tube for, and in, vapor compression systems. *ASHRAE Trans.* 91, 92–103.
- Seixlack, A.L., 1996. Modeling the HFC 134a Flow Through Capillary Tubes Using a Two-Fluid Model, in: *International Refrigeration and Air Conditioning Conference*. Purdue.
- Seixlack, A.L., Barbazelli, M.R., 2009. Numerical analysis of refrigerant flow along non-adiabatic capillary tubes using a two-fluid model. *Appl. Therm. Eng.*

- <https://doi.org/10.1016/j.applthermaleng.2008.03.012>
- Tannert, T., Hesse, U., 2016. Noise Effects In Capillary Tubes Caused By Refrigerant Flow, in: International Refrigeration and Air Conditioning Conference. Purdue.
- Taylor, G.I., 1960. The rear meniscus of a long bubble steadily displacing a Newtonian liquid in a capillary tube. *J. Fluid Mech.* 10, 161–165.
- Wang, J., Cao, F., Wang, Z., Zhao, Y., Li, L., 2012. Numerical simulation of coiled adiabatic capillary tubes in CO₂ transcritical systems with separated flow model including metastable flow. *Int. J. Refrig.* <https://doi.org/10.1016/j.ijrefrig.2012.07.012>
- Weisman, J., 1983. Two-Phase Flow Patterns, In *Handbook of Fluids in Motion*. Ann Arbor Science Publishers, Ann Arbor.
- Wong, T.N., Ooi, K.T., 1996. Adiabatic capillary tube expansion devices: a comparison of the homogeneous flow and the separated flow models. *Appl. Therm. Eng.* 16, 625–634.
- Wongwises, S., Pirompak, W., 2001. Flow characteristics of pure refrigerants and refrigerant mixtures in adiabatic capillary tubes. *Appl. Therm. Eng.* [https://doi.org/10.1016/S1359-4311\(00\)00090-9](https://doi.org/10.1016/S1359-4311(00)00090-9)
- Xu, B., Bansal, P., 2002. Non-adiabatic capillary tube flow: a homogeneous model and process description. *Appl. Therm. Eng.* 22, 1801–1819. [https://doi.org/10.1016/S1359-4311\(02\)00110-2](https://doi.org/10.1016/S1359-4311(02)00110-2)

7. Acknowledgments

This work was financially supported by the Slovenian Research Agency as part of the Young Researcher PhD program.